Article

Bistridentate Ruthenium(II)polypyridyl-Type Complexes with Microsecond MLCT State Lifetimes: Sensitizers for Rod-Like Molecular Arrays

Maria Abrahamsson, Michael Ja#ger, Rohan J. Kumar, Tomas O#sterman, Petter Persson, Hans-Christian Becker, Olof Johansson, and Leif Hammarstro#m

J. Am. Chem. Soc., **2008**, 130 (46), 15533-15542 • DOI: 10.1021/ja804890k • Publication Date (Web): 29 October 2008

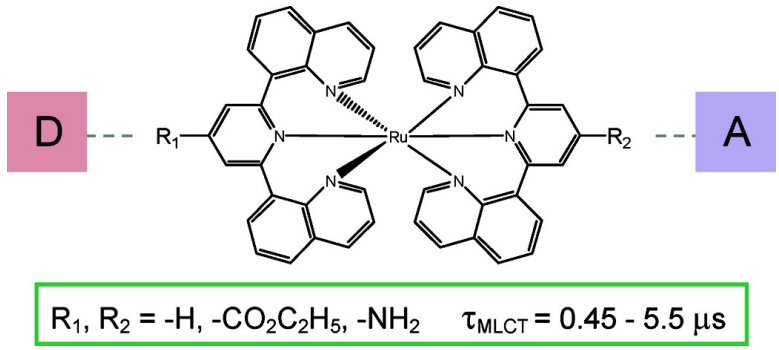

More About This Article

Additional resources and features associated with this article are available within the HTML version:

- Supporting Information
- Access to high resolution figures
- Links to articles and content related to this article
- Copyright permission to reproduce figures and/or text from this article

View the Full Text HTML

J|A|C|S
ARTICLES

Published on Web 10/29/2008

Bistridentate Ruthenium(II)polypyridyl-Type Complexes with Microsecond ^{3}MLCT State Lifetimes: Sensitizers for Rod-Like Molecular Arrays

Maria Abrahamsson,[†,‡] Michael Jäger,[†] Rohan J. Kumar,[†] Tomas Österman,[§,||] Petter Persson,[§,||] Hans-Christian Becker,[†] Olof Johansson,*[,†] and Leif Hammarström*[,†]

Department of Photochemistry and Molecular Science, The Ångström Laboratories, Uppsala University, Box 523, SE-751 20 Uppsala, Sweden, Department of Quantum Chemistry, Uppsala University, Box 518, SE-751 20, Uppsala, Sweden, and Department of Chemical Physics, Lund University, Box 124, SE-221 00 Lund, Sweden

Received June 26, 2008; E-mail: Olof.Johansson@fotomol.uu.se; Leif@fotomol.uu.se

Abstract: A series of bistridentate ruthenium(II) polypyridyl-type complexes based on the novel 2,6-di(quinolin-8-yl)pyridine (dqp) ligand have been synthesized and their photophysical properties have been studied. The complexes are amenable to substitution in the 4-position of the central pyridine with conserved quasi-C_{2v} symmetry, which allows for extension to isomer-free, rod-like molecular arrays for vectorial control of electron and energy transfer. DFT calculations performed on the parent $[Ru(dqp)_2]^{2+}$ complex (**1**) predicted a more octahedral structure than in the typical bistridentate complex $[Ru(tpy)_2]^{2+}$ (tpy is 2,2′:6′,2″-terpyridine) thanks to the larger ligand bite angle, which was confirmed by X-ray crystallography. A strong visible absorption band, with a maximum at 491 nm was assigned to a metal-to-ligand charge transfer (MLCT) transition, based on time-dependent DFT calculations. **1** shows room temperature emission ($\Phi = 0.02$) from its lowest excited (^{3}MLCT) state that has a very long lifetime ($\tau = 3$ μs). The long lifetime is due to a stronger ligand field, because of the more octahedral structure, which makes the often dominant activated decay via short-lived metal-centered states insignificant also at elevated temperatures. A series of complexes based on dqp with electron donating and/or accepting substituents in the 4-position of the pyridine was prepared and the properties were compared to those of **1**. An unprecedented ^{3}MLCT state lifetime of 5.5 μs was demonstrated for the homoleptic complex based on dqpCO_2Et. The favorable photosensitizer properties of **1**, such as a high extinction coefficient, high excited-state energy and long lifetime, and tunable redox potentials, are maintained upon substitution. In addition, the parent complex **1** is shown to be remarkably photostable and displays a high reactivity in light-induced electron and energy transfer reactions with typical energy and electron acceptors and donors: methylviologen, tetrathiofulvalene, and 9,10-diphenylanthracene. This new class of complexes constitutes a promising starting point for the construction of linear, rod-like molecular arrays for photosensitized reactions and applications in artificial photosynthesis and molecular electronics.

Introduction

Molecular assemblies based on ruthenium(II)polypyridyl complexes continue to attract large interest in the context of photochemical solar energy conversion and molecular electronics.[1] Their favorable use in, for example, light-induced electron and energy transfer reactions derive from the properties of the lowest excited triplet metal-to-ligand charge transfer (^{3}MLCT) state that often has a lifetime as long as 100−1000 ns. Most often, a vectorial transfer of electrons or excitation energy is desired to exercise control over these processes on a nanometer scale. Although $[Ru(bpy)_3]^{2+}$ (bpy is 2,2′-bipyridine) and derivatives thereof have been widely used as the photoactive component in such assemblies, they typically give rise to a range of isomers in which electron and energy transfer processes do not proceed with a well-defined directionality (Scheme 1). Instead, it has long since been recognized[1c,2] that complexes based on tridentate ligands such as 2,2′:6′,2″-terpyridine (tpy) are much more attractive due to the inherent linearity and isomeric purity obtained in multiunit assemblies with substitution along the C_2 axis, that is in the 4′-position of tpy ligands.

[†] The Ångström Laboratories, Uppsala University.
[‡] Present address: Department of Chemistry, Johns Hopkins University, Baltimore, MD, 21218.
[§] Department of Quantum Chemistry, Uppsala University.
[||] Department of Chemical Physics, Lund University.

(1) (a) Scandola, F.; Chiorboli, C.; Indelli, M. T.; Rampi, M. *Electron Transfer in Chemistry*; Wiley: Weinheim, 2001; p 337. (b) Alstrum-Acevedo, J. H.; Brennaman, M. K.; Meyer, T. J. *Inorg. Chem.* **2005**, *44*, 6802–6827. (c) Sauvage, J. P.; Collin, J. P.; Chambron, J. C.; Guillerez, S.; Coudret, C.; Balzani, V.; Barigelletti, F.; Decola, L.; Flamigni, L. *Chem. Rev.* **1994**, *94*, 993–1019. (d) Barigelletti, F.; Flamigni, L. *Chem. Soc. Rev.* **2000**, *29*, 1–12. (e) Sun, L. C.; Hammarström, L.; Åkermark, B.; Styring, S. *Chem. Soc. Rev.* **2001**, *30*, 36–49.

(2) Maestri, M.; Armaroli, N.; Balzani, V.; Constable, E. C.; Thompson, A. *Inorg. Chem.* **1995**, *34*, 2759–2767.

Scheme 1 [a]

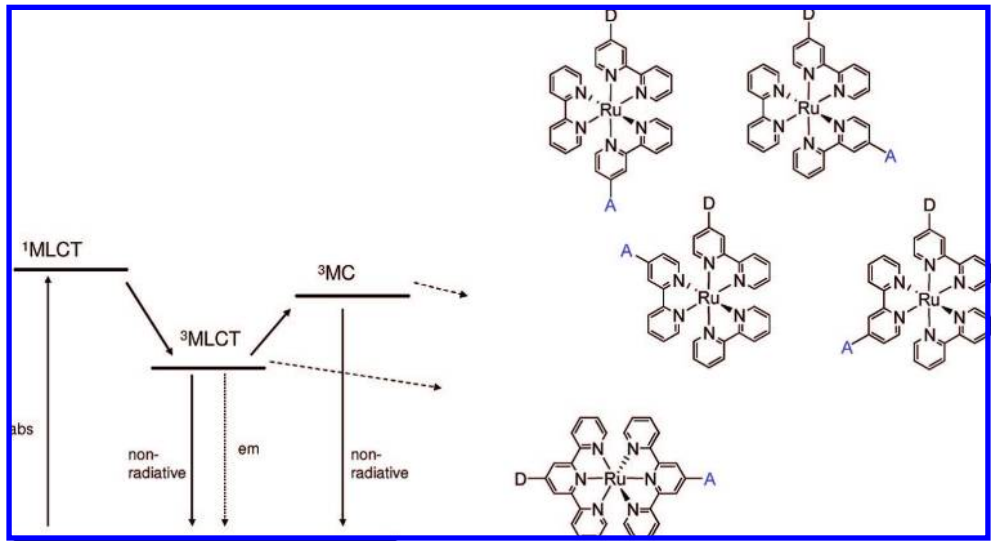

[a] (Left) Excited state diagram for typical ruthenium(II)polypyridine complexes, showing the relevant deactivation pathways of the emissive ^{3}MLCT state[10] at room temperature (see text). Dashed lines denote photochemical reactions, which for the ^{3}MLCT state may be e.g. electron- and energy transfer, while the ^{3}MC state rather undergoes rapid deactivation or ligand substitution. (Right) Diastereomers of a donor-acceptor substituted $Ru^{II}(bpy)_3$-complex (the additional enantiomeric forms are not shown), and the single isomer of the corresponding donor-$Ru^{II}(tpy)_2$-acceptor complex (adapted from ref 11).

However, the $[Ru(tpy)_2]^{2+}$ prototype has an excited-state lifetime of only 0.25 ns at room temperature,[1c,2] which makes it less useful for photosensitizer applications. The short lifetime is due to rapid deactivation of the emissive, lowest excited ^{3}MLCT state via thermal population of short-lived and nonemissive triplet metal-centered (^{3}MC) states (Scheme 1).[3] Much attention has therefore been focused on the design and synthesis of new bistridentate ruthenium(II) complexes with extended lifetimes. These strategies include the use of (1) electron accepting and/or donating substituents,[2,4,5] (2) ligands with extended π-systems,[4,6] (3) cyclometalating or other strong σ-donor ligands,[4,7] and (4) bichromophoric systems.[4,8] The first three approaches are based on the fact that an increased energy gap between the lowest excited ^{3}MLCT state and the ^{3}MC states would lead to slower population of the latter, and thus a prolonged excited-state lifetime. This has generally resulted in a lower ^{3}MLCT state energy, however, which makes the complexes less useful in photosensitizer applications, and the substituents frequently block the 4′-position of the parent tpy ligand for further derivatization. In the bichromophoric approach instead, a low energy $\pi \rightarrow \pi^*$ state of an appended organic chromophore serves as a reservoir leading to repopulation of the emissive ^{3}MLCT state with a concomitant increase in the observed emission lifetime (analogous to delayed fluorescence). As we pointed out before,[9] the actual ^{3}MLCT lifetime is not increased, however. The reason for the long-lived emission is instead the very low degree of ^{3}MLCT state population, but therefore its photochemical reactivity is decreased to the same degree as the apparent lifetime is increased. This is illustrated by the fact that the yield of ^{3}MLCT emission is not increased by appending the triplet reservoir unit.[8a] This approach is thus not a viable way of increasing the lifetime and photochemical reactivity of the ^{3}MLCT state, but rather of interest for intramolecular triplet sentitization of the organic chromophore.

(3) (a) Meyer, T. J. *Pure Appl. Chem.* **1986**, *58*, 1193. (b) Juris, A.; Balzani, V.; Barigelletti, F.; Campagna, S.; Belser, P.; Von Zelewsky, A. *Coord. Chem. Rev.* **1988**, *84*, 85–277.
(4) (a) Medlycott, E. A.; Hanan, G. S. *Coord. Chem. Rev.* **2006**, *250*, 1763–1782. (b) Medlycott, E. A.; Hanan, G. S. *Chem. Soc. Rev.* **2005**, *34*, 133–142.
(5) (a) Wang, J. H.; Fang, Y. Q.; Hanan, G. S.; Loiseau, F.; Campagna, S. *Inorg. Chem.* **2005**, *44*, 5–7. (b) Constable, E. C.; Cargill Thompson, A. M. W.; Armaroli, N.; Balzani, V.; Maestri, M. *Polyhedron* **1992**, *11*, 2707–2709.
(6) (a) Polson, M. I. J.; Loiseau, F.; Campagna, S.; Hanan, G. S. *Chem. Comm.* **2006**, 1301–1303. (b) Polson, M. I. J.; Medlycott, E. A.; Hanan, G. S.; Mikelsons, L.; Taylor, N. L.; Watanabe, M.; Tanaka, Y.; Loiseau, F.; Passalacqua, R.; Campagna, S. *Chem.−Eur. J.* **2004**, *10*, 3640–3648. (c) Fang, Y. Q.; Taylor, N. J.; Hanan, G. S.; Loiseau, F.; Passalacqua, R.; Campagna, S.; Nierengarten, H.; Van Dorsselaer, A. *J. Am. Chem. Soc.* **2002**, *124*, 7912–7913. (d) Encinas, S.; Flamigni, L.; Barigelletti, F.; Constable, E. C.; Housecroft, C. E.; Schofield, E. R.; Figgemeier, E.; Fenske, D.; Neuburger, M.; Vos, J. G.; Zehnder, M. *Chem.−Eur. J.* **2002**, *8*, 137–150. (e) Ceroni, P.; Credi, A.; Balzani, V.; Campagna, S.; Hanan, G. S.; Arana, C. R.; Lehn, J. M. *Eur. J. Inorg. Chem.* **1999**, 1409–1414. (f) Hissler, M.; El-ghayoury, A.; Harriman, A.; Ziessel, R. *Angew. Chem., Int. Ed.* **1998**, *37*, 1717–1720. (g) Hammarström, L.; Barigelletti, F.; Flamigni, L.; Indelli, M. T.; Armaroli, N.; Calogero, G.; Guardigli, M.; Sour, A.; Collin, J. P.; Sauvage, J. P. *J. Phys. Chem. A.* **1997**, *101*, 9061–9069.
(7) (a) Son, S. U.; Park, K. H.; Lee, Y. S.; Kim, B. Y.; Choi, C. H.; Lah, M. S.; Jang, Y. H.; Jang, D. J.; Chung, Y. K. *Inorg. Chem.* **2004**, *43*, 6896–6898. (b) Duati, M.; Tasca, S.; Lynch, F. C.; Bohlen, H.; Vos, J. G.; Stagni, S.; Ward, M. D. *Inorg. Chem.* **2003**, *42*, 8377–8384. (c) Duati, M.; Fanni, S.; Vos, J. G. *Inorg. Chem. Commun.* **2000**, *3*, 68–70. (d) Indelli, M. T.; Bignozzi, C. A.; Scandola, F.; Collin, J. P. *Inorg. Chem.* **1998**, *37*, 6084–6089. (e) Constable, E. C.; Thompson, A. M. W.; Cherryman, J.; Liddiment, T. *Inorg. Chim. Acta* **1995**, *235*, 165–171. (f) Collin, J. P.; Beley, M.; Sauvage, J. P.; Barigelletti, F. *Inorg. Chim. Acta* **1991**, *186*, 91–93.
(8) (a) McClenaghan, N. D.; Leydet, Y.; Maubert, B.; Indelli, M. T.; Campagna, S. *Coord. Chem. Rev.* **2005**, *249*, 1336–1350. (b) Wang, X. Y.; Del Guerzo, A.; Schmehl, R. H. *J. Photochem. Photobiol. C* **2004**, *5*, 55–77. (c) Wang, J. H.; Hanan, G. S.; Loiseau, F.; Campagna, S. *Chem. Comm.* **2004**, 2068–2069. (d) Passalacqua, R.; Loiseau, F.; Campagna, S.; Fang, Y. Q.; Hanan, G. S. *Angew. Chem., Int. Ed.* **2003**, *42*, 1608–1611. (e) Baba, A. I.; Shaw, J. R.; Simon, J. A.; Thummel, R. P.; Schmehl, R. H. *Coord. Chem. Rev.* **1998**, *171*, 43–59.
(9) Abrahamsson, M.; Jäger, M.; Österman, T.; Eriksson, L.; Persson, P.; Becker, H. C.; Johansson, O.; Hammarström, L. *J. Am. Chem. Soc.* **2006**, *128*, 12616–12617.
(10) For the parent complex $[Ru(bpy)_3]^{2+}$ at least three ^{3}MLCT states within 60 cm^{-1} in energy are in rapid thermal equilibrium at room temperature and constitute "the lowest ^{3}MLCT state"; see:(a) Crosby, G. A. *Acc. Chem. Res.* **1975**, *8*, 231.

Chart 1. Structure of the Complexes Studied

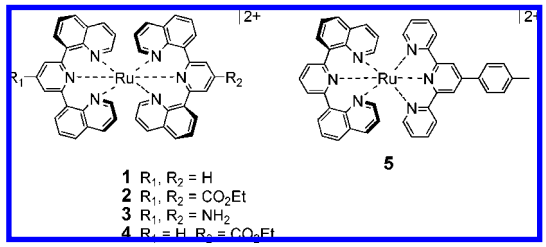

We have previously reported on an alternative strategy to prolong the excited-state lifetime in bistridentate ruthenium(II)polypyridyl complexes.[9,12] It is well recognized that the small bite angle of the tpy ligands gives a weak ligand field and hence a smaller ^{3}MLCT-^{3}MC energy gap in $[Ru(tpy)_2]^{2+}$ than in $[Ru(bpy)_3]^{2+}$. We reasoned, therefore, that the design of tridentate ligands that allow for larger bite angles would result in more octahedral complexes and consequently longer excited-state lifetimes without necessarily lowering the excited-state energy. By introducing a methylene group between two pyridines in the tpy ligand to give an unsymmetrical bpy-CH_2-py ligand, the excited-state lifetime of the homoleptic ruthenium(II) complex increased to 15 ns, but the complex showed degradation under irradiation.[12a] A comparison with a homoleptic ruthenium(II) complex with bpy-$C(CH_3)_2$-py ligands furthermore showed that the excited states lifetime for complexes with such flexible ligands are very sensitive to steric interactions influencing the ligand field splitting through modification of the metal co-ordination geometry.[13] Recently, we extended this concept and reported a major improvement via the design and synthesis of 2,6-di(quinolin-8-yl)pyridine (dqp) and the corresponding homoleptic ruthenium(II) complex $[Ru(dqp)_2]^{2+}$ (**1**; see Chart 1).[9] The ligand is less flexible than, for example, bpy-CH_2-py, the structure involves only 6-membered chelates, and the geometry around the ruthenium ion is close to octahedral. Most importantly, it displays an excited-state lifetime of 3.0 μs at room temperature. Also, the 4-positions on the central pyridines are available for substitution and future preparation of linear donor−chromophore−acceptor arrays.

We now report a full study of the excited-state and photosensitizer properties of **1**, including a demonstration of its high photostability and usefulness in electron- and energy transfer reactions. In addition a series of ruthenium(II) complexes based on substituted dqp ligands is presented (Chart 1), with electron donating (-NH_2) and electron accepting (-CO_2Et) substituents available for further functionalization, and their properties are compared to those of the parent complex. Our results show that these complexes combine an optimal geometry for extension to rod-like molecular arrays with excellent photosensitizer properties, such as a long excited-state lifetime, good excited-state electron and energy transfer properties, and very good photostability. We thus demonstrate that these complexes are useful photosensitizers for many applications.

Results and Discussion

Synthesis and Structure. Before **1** was synthesized quantum chemical calculations were performed to investigate its structural and electronic properties. As the results suggested an almost octahedral coordination and suitable electronic properties (see below), the ligands and complexes were synthesized.

The ligands 2,6-di(quinolin-8-yl)pyridine (dqp) and 4-ethylcarboxy-2,6-di(quinolin-8-yl)pyridine (dqpCO_2Et) were synthesized in high yields via the Suzuki-Miyaura cross-coupling reaction from commercially available quinoline-8-boronic acid and the appropriate dihalopyridine. 4-Amino-2,6-di(quinolin-8-yl)pyridine (dqpNH_2) was conveniently prepared via reduction of 4-nitro-2,6-di(quinolin-8-yl)pyridine.[9,14]

In the synthesis of the dqp-based ruthenium(II) complexes in this study, we adopted the procedures often used for the related bisterpyridyl complexes.[15] The homoleptic complex **1** was synthesized in 87% yield by the reaction of two equivalents of dqp with $Ru(DMSO)_4Cl_2$ in ethylene glycol at 200 °C for 20 min using microwave heating (Scheme 2).[9] Using the same conditions with dqpNH_2 resulted in a 22% isolated yield of complex **3**. However, applying the same protocol with dqpCO_2Et gave only minute quantities of complex **2**. We observed a pressure rise and complex **1**, formed via a decarboxylation reaction,[16] was detected in the crude product by LC-MS. The synthesis of complex **2** was instead accomplished in 20% yield by the reaction of $RuCl_3 \cdot 3H_2O$ and two equivalents of dqpCO_2Et with *N*-ethylmorpholine as a reductant in refluxing EtOH. The heteroleptic complexes **4** and **5** were obtained using a stepwise procedure. Reacting Ru(ttpy)Cl_3 (ttpy is 4′-(p-tolyl)-2,2′:6′,2″-terpyridine) and Ru(dqp)Cl_3 (refluxing EtOH with added *N*-ethylmorpholine) with dqp and dqpCO_2Et, respectively, gave **4** and **5** in modest yields. Multiple unidentified colored byproducts, presumably other ruthenium complexes, were always observed when complexation was performed at lower temperatures (80−100 °C). The desired complexes therefore required careful and repeated purification by column chromatography which reduces isolated yields. In general, high yields are not obtained by direct application of the procedures commonly used for the ruthenium(II) bisterpyridyl analogues. Given the high potential of the dqp-based ruthenium(II) complexes in energy conversion schemes, we have therefore initiated a detailed study of the coordination of these ligands that will be reported in due course.

The DFT results for **1** suggested meridional co-ordination of the dqp ligands and a co-ordination geometry that was close to octahedral with regular Ru−N bond distances (Table 1). The X-ray crystal structure was later proven to be very similar to the calculated structure with an experimentally determined N1−Ru−N3 bite angle of 178°, very close to the ideal value of 180° for an octahedral complex (Table 1).[9] It is a substantial

(11) Baranoff, E.; Collin, J.-P.; Flamigni, L.; Sauvage, J.-P. *Chem. Soc. Rev.* **2004**, *33*, 147–155.
(12) (a) Abrahamsson, M.; Wolpher, H.; Johansson, O.; Larsson, J.; Kritikos, M.; Eriksson, L.; Norrby, P. O.; Bergquist, J.; Sun, L. C.; Akermark, B.; Hammarstrom, L. *Inorg. Chem.* **2005**, *44*, 3215–3225. (b) Wolpher, H.; Johansson, O.; Abrahamsson, M.; Kritikos, M.; Sun, L. C.; Akermark, B. *Inorg. Chem. Commun.* **2004**, *7*, 337–340.
(13) Abrahamsson, M.; Lundqvist, M. J.; Wolpher, H.; Johansson, O.; Eriksson, L.; Bergquist, J.; Rasmussen, T.; Becker, H.-C.; Hammarström, L.; Norrby, P.-O.; Åkermark, B.; Persson, P. *Inorg. Chem.* **2008**, *47*, 3540–3548.
(14) Jäger, M.; Eriksson, L.; Bergquist, J.; Johansson, O. *J. Org. Chem.* **2007**, *72*, 10227–10230.
(15) For a general introduction to the synthesis of bisterpyridyl ruthenium(II) complexes, see:(a) Hofmeier, H.; Schubert, U. S. *Chem. Soc. Rev.* **2004**, *33*, 373–399. (b) Schubert, U. S.; Hofmeier, H.; Newkome, G. R. *Modern Terpyridine Chemistry*; WILEY-VCH: Weinheim, 2006.
(16) It has recently been reported that 2,2′-bipyridinyl-4,4′-dicarboxylic acid diethyl ester readily decarboxylates during Ru complexation using microwave heating with $RuCl_3$ as precursor; see:(a) Anderson, T. J.; Scott, J. R.; Millett, F.; Durham, B. *Inorg. Chem.* **2006**, *45*, 3843–3845.

Scheme 2

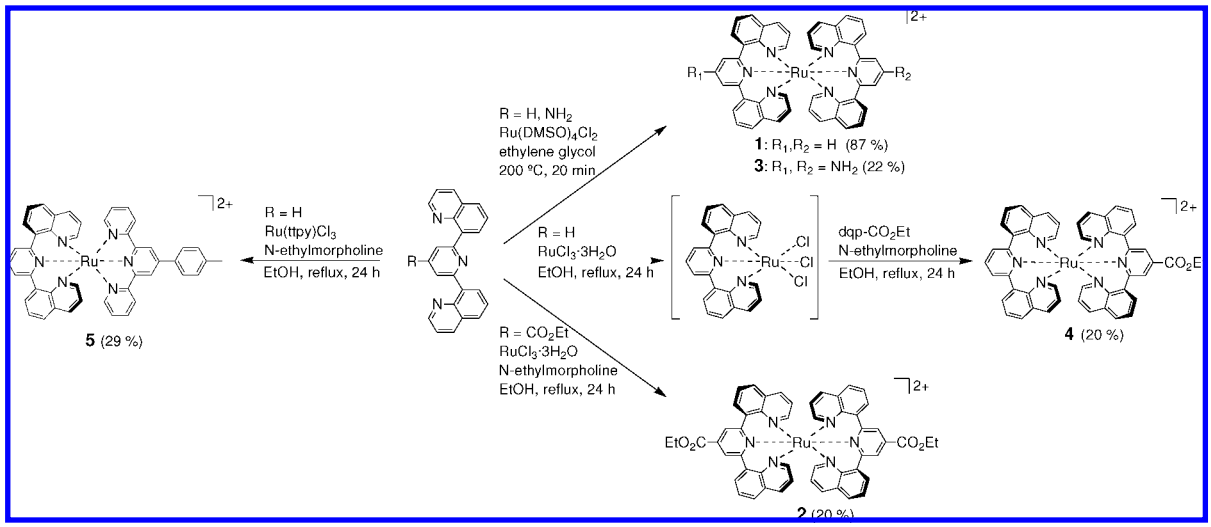

Table 1. Selected Calculated Ru−N Bond Lengths (Å) and N−Ru−N angles (degrees) for **1**, and Corresponding Experimental Values for **1** and $[Ru(tpy)_2]^{2+}$ (Numbering of N Atoms As in Chart 2)[a]

	calculated structure for **1**			experimental	
	LANL2DZ	6−31G	6−31G(d,p)[b]	**1**	$[Ru(tpy)_2]^{2+}$[c]
Ru−N1	2.114	2.124	2.120	2.077	2.067
Ru−N2	2.081	2.089	2.085	2.025	1.981
N1−Ru−N2	89.8	89.5	89.5	92.1	79.5
N1−Ru−N3	179.6	179.0	179.0	177.6	158.4
N2−Ru−N5	180.0	180.0	180.0	176.3	178.8

[a] The optimizations were performed using the B3LYP hybrid exchange-correlation functional together with the basis set listed in the table for H, C, and N. In all cases, Ru was described with LANL2DZ. [b] B3LYP calculations employing 6−31G(d,p) for 1st and 2nd row atoms and SDD for Ru (see ref 20). [c] See ref 17.

improvement over the 158° bite angle found in $[Ru(tpy)_2]^{2+}$[17] and shows that the design strategy was successful. In agreement with the calculated structure, the X-ray structure shows twisted arrangements of both dqp ligands with dihedral angles between the central pyridine and the quinoline units that are 35−39°. The twisted structure is stabilized by interligand $\pi-\pi$ interactions between two quinoline units forming two pairs of quinolines, each with an interplanar distance of about 3.5 Å.[14] In Table 1, selected structural parameters from DFT geometry optimizations are compared to the experimentally determined structures of **1** and $[Ru(tpy)_2]^{2+}$. There is overall good agreement for all basis sets, in particular the intraligand bond lengths. The largest deviations are observed for the Ru−N bond lengths, which are systematically overestimated by up to 0.07 Å in the B3LYP calculations with all basis sets. This behavior is expected from calculations on similar complexes.[18] The remaining discrepancies between the calculated and the experimental structure may be related to shortcomings of the B3LYP functional, but are evidently not due to basis set limitations as the Ru−N bond lengths calculated using the 6−31+G(d,p) all-electron basis set with diffuse and polarization functions for all atoms on the ligands are actually in slightly worse agreement with the experimental structure compared to the LANL2DZ basis set with effective core potentials where the Ru−N bond lengths are only overestimated by 0.043 Å on average. N−Ru−N angles are typically described by the various methods to within 4 degrees, which is compatible with the expected accuracy of the employed DFT methodology.[19] Overall, the results from DFT calculations are in very good agreement with the experimentally determined structure. This provides *a posteriori* confirmation of the initial B3LYP/LANL2DZ predictions of the structural properties of new classes of ruthenium(II) polypyridyl-type complexes.

Chart 2. Numbering of N Atoms in Table 1

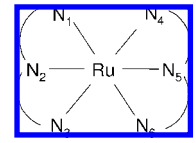

The solution structures were analyzed by ^{1}H NMR and all complexes showed well-resolved ^{1}H NMR spectra (Supporting Information) where the proton signals could be assigned using two-dimensional spectroscopy. In complexes **1**−**4**, the chemical shifts of all quinoline protons are significantly upfield shifted upon co-ordination compared to the free ligands due to intramolecular stacking of the quinoline units in agreement with the X-ray crystal structure of **1**.[14] In contrast, the ^{1}H NMR of complex **5** that has one 2,2′:6′,2″-terpyridine ligand is distinctly different as the planarity of the terpyridine prevents interligand $\pi-\pi$ interactions (Supporting Information).

Electrochemistry. The redox potentials for all complexes were determined by cyclic voltammetry (CV) in CH_3CN and are reported in Table 2 (vs $Fc^{+/0}$). Good reversibility was obtained, as judged from the peak heights on the reverse scans and from the small split of reduction and oxidation peaks (ΔE_p). In some cases adsorption peaks for the reduced complexes were obtained in the CVs and the peak potentials from differential pulse voltammetry (DPV) are reported instead. Assignments of the redox processes were made in analogy with the rich literature on ruthenium(II) polypyridyl complexes, and were in the case of **1** supported by the HOMO and LUMO electronic structure from DFT calculations (see below). Complex **1** showed a

(17) Lashgari, K.; Kritikos, M.; Norrestam, R.; Norrby, T. *Acta Cryst. Sec. C* **1999**, 64–67.
(18) Gorelsky, S. I.; Lever, A. B. P. *J. Organomet. Chem.* **2001**, *635*, 187–196.
(19) Cramer, C. J. *Essentials of Computational Chemistry: Theories and Models*; John Wiley & Son, Ltd: Leicester, 2002.

Table 2. Absorption and Electrochemical Properties of the Complexes in CH_3CN

	Absorption peak/nm ($\varepsilon \times 10^{-4}$/M^{-1}cm^{-1})	$E_{1/2}$/V[a] (ΔE_p[b]/ mV)		
		$Ru^{III/II}$	$L^{0/-}$	$L^{-/2-}$
1	491 (1.4), 336 (3.1), 281 (3.3)	+0.71 (63)	−1.73 (62)	−1.90[c]
2	553 (1.0), 488 (1.1), 361 (2.7), 268 (3.0)	+0.82 (69)	−1.52 (65)	−1.73 (66)
3	563 (0.8), 476 (1.1), 401 (0.7), 321 (2.6)	+0.34 (72)	−1.86 (75)[d]	−2.03 (71)[d]
4	549 (0.7), 492 (1.0), 345 (1.9), 278 (2.4)	+0.77 (77)	−1.58 (74)	−1.89 (84)
5	570 (0.9), 526 (1.4), 457 (1.5), 322 (6.4), 285 (6.1)	+0.78 (72)	−1.55[c]	− 1.76[c]
$[Ru(tpy)_2]^{2+}$	476 (1.8), 308 (6.4), 272 (3.8)	+0.92[e]	−1.62[e]	

[a] From CV in 0.1 M $TBAPF_6$, CH_3CN, 0.1 V/s, vs $Fc^{+/0}$. [b] Difference between anodic and cathodic peak potentials. [c] DPV peak potential. [d] Recorded at 1 V/s (irreversible at 0.1 V/s), not corrected for IR drop. [e] Reference 1c. Potentials reported vs SSCE, 0.375 V subtracted to obtain values vs $Fc^{+/0}$.

reversible one-electron $Ru^{III/II}$ oxidation at $E_{1/2} = +0.71$ V which is lower than in $[Ru(tpy)_2]^{2+}$ ($E_{1/2} = +0.92$ V). Considering the similar pK_a values for quinoline and pyridine, 4.94 and 5.20 respectively,[21] this indicates less efficient π back-bonding in **1** than in $[Ru(tpy)_2]^{2+}$.[22] A reversible, ligand-based, one-electron reduction occurs at $E_{1/2} = -1.73$ V ($E_{1/2} = -1.62$ V for $[Ru(tpy)_2]^{2+}$). The heteroleptic complex **5** containing a ttpy ligand showed a metal-based oxidation at intermediate potential ($E_{1/2} = +0.78$ V), while the first ligand-based reduction occurs at less negative potential ($E_{1/2} = -1.55$ V) than in **1**, suggesting a ttpy-based reduction.

The 4-substituted complexes **2**−**4** follow the expected trend for similar ruthenium(II) polypyridyl complexes where the $Ru^{III/II}$ redox couple and the ligand-based reductions vary with the donor/acceptor properties of the substituents.[2,23] The electron withdrawing -CO_2Et substituents in **2** and **4** shift the $Ru^{III/II}$ potential to more positive values, while complex **3** containing the electron-donating amines is much more easily oxidized (Table 2). The good reversibility of the oxidation of **3** supports the assignment to a metal-centered oxidation rather than oxidation of the amine groups. This assignment is also supported by the parallel shifts of emission energy and redox potentials, see below. The one-electron reductions in **2** and **4** occur at less negative potentials than in **1** while complex **3** is reduced at a more negative potential.

Electronic Structure and Absorption Spectra. The electronic structure of **1** has been characterized from DFT and TD-DFT calculations using B3LYP/LANL2DZ with a PCM description for the solvent (ethanol). The three highest occupied molecular orbitals (HOMOs) are nearly degenerate and of essentially pure Ru 4d (t_{2g}) character (Figure 1a), which is typical for octahedral ruthenium(II) polypyridyl complexes.[3] The three lowest unoccupied molecular orbitals (LUMOs) are instead ligand centered π^* orbitals that have only minor contributions from the central ruthenium (Figure 1b−d). This supports the assignments of the electrochemical processes above. In view of the potential applications of the $[Ru(dqp)_2]^{2+}$ complexes as chromophores in linear arrays, it is interesting to note that the LUMO in **1** has significant contribution from the 4-pyridine position of dqp. In contrast, both LUMO+1 and LUMO+2 have little or no contributions from this position due to the nodal structure of these orbitals. These differences are likely to significantly influence the electronic coupling to neighboring functional units via these particular molecular orbitals.

The UV−vis absorption spectra for the complexes in CH_3CN are shown in Figure 2, and the data is summarized in Table 2. All complexes display transitions in the UV-region, with a strong band around 230 nm and somewhat weaker ones around 270−280 nm and 315−360 nm. The bands around 230 nm and 315−360 nm are present also in the free ligand absorption spectra, although they red-shift by 10−20 nm upon complexation, and are therefore attributed to ligand centered (LC) transitions. In the visible region the expected $d\pi \rightarrow \pi^*$ ^{1}MLCT bands dominate the spectra. This absorption is strong for all complexes ($\varepsilon_{max} = (1.0 - 1.5) \times 10^4$ M^{-1}cm^{-1}), with a maximum around 480−490 nm for **1**−**4** while **5** (and to some extent **2**) shows several more resolved peaks in the same region.

Important support for the assignment of the absorption spectra of **1** is given by the TD-DFT calculations. Vertical excitation energies, oscillator strengths, and assignments of the types of transitions are given for selected excitations in Table 3. A comparison of the calculated excitations with the measured visible absorption spectrum shows that there is a good general agreement.[9] The broad absorption band around 490 nm, and an onset of a stronger absorption band starting at 390 nm are well matched by the TD-DFT calculations both in terms of position and relative intensity. The calculations indicate that the low energy absorption band around 490 nm is largely composed of MLCT excitations, with some contributions on the high-energy side from MC excitations. Strong LC $\pi \rightarrow \pi^*$ excitations contribute to the intense band starting at 390 nm. The lowest excited states are MLCT states resulting from excitation from the Ru 4d HOMOs to the dqp LUMOs. For example, the first excited singlet state with a calculated vertical excitation wavelength of 538 nm is dominated by a transition from the HOMO to the LUMO shown in Figure 1a and b, respectively. Some further information about calculated potential energy surfaces for the lowest excited triplet state relevant for ^{3}MLCT$\rightarrow^3$MC conversion were recently discussed for Ru(II) bis-tridentate complexes including $[Ru(dqp)_2]^{2+}$.[20]

Emission and Excited-State Properties. The emission and excited-state properties of **1**−**5** were investigated in view of establishing the potential of these new complexes as photosensitizers. In sharp contrast to typical bistridentate Ru^{II} complexes such as $[Ru(tpy)_2]^{2+}$, complex **1**, **2**, and **4** all show fairly strong emission in room temperature solution, with a maximum around 700 nm (Table 4). The good emission yield is matched by exceptionally long excited-state lifetimes. We have previously reported the excited-state lifetime of 3.0 μs for **1**, which was the longest ^{3}MLCT lifetime at room temperature reported for any ruthenium(II) polypyridyl complex (see Introduction). Now we present even longer lifetimes for **2** and **4**,

(20) Borg, O. A.; Godinho, S. S. M. C.; Lundqvist, M. J.; Lunell, S.; Persson, P. *J. Phys. Chem. A* **2008**, *112*, 4470–4476.
(21) Lokhov, R. E. *Chem. Heterocycl. Compd.* **1981**, *17*, 72.
(22) Juris, A.; Belser, P.; Barigelletti, F.; Von Zelewsky, A.; Balzani, V. *Inorg. Chem.* **1986**, *25*, 256–259.
(23) (a) Constable, E. C.; Cargill Thompson, A. M. W.; Tocher, D. A.; Daniels, M. A. M. *New J. Chem.* **1992**, *16*, 855–867. (b) Fallahpour, R. A.; Neuburger, M.; Zehnder, M. *New J. Chem.* **1999**, 53. (c) Fallahpour, R. A. *Eur. J. Inorg. Chem.* **1998**, 1205.

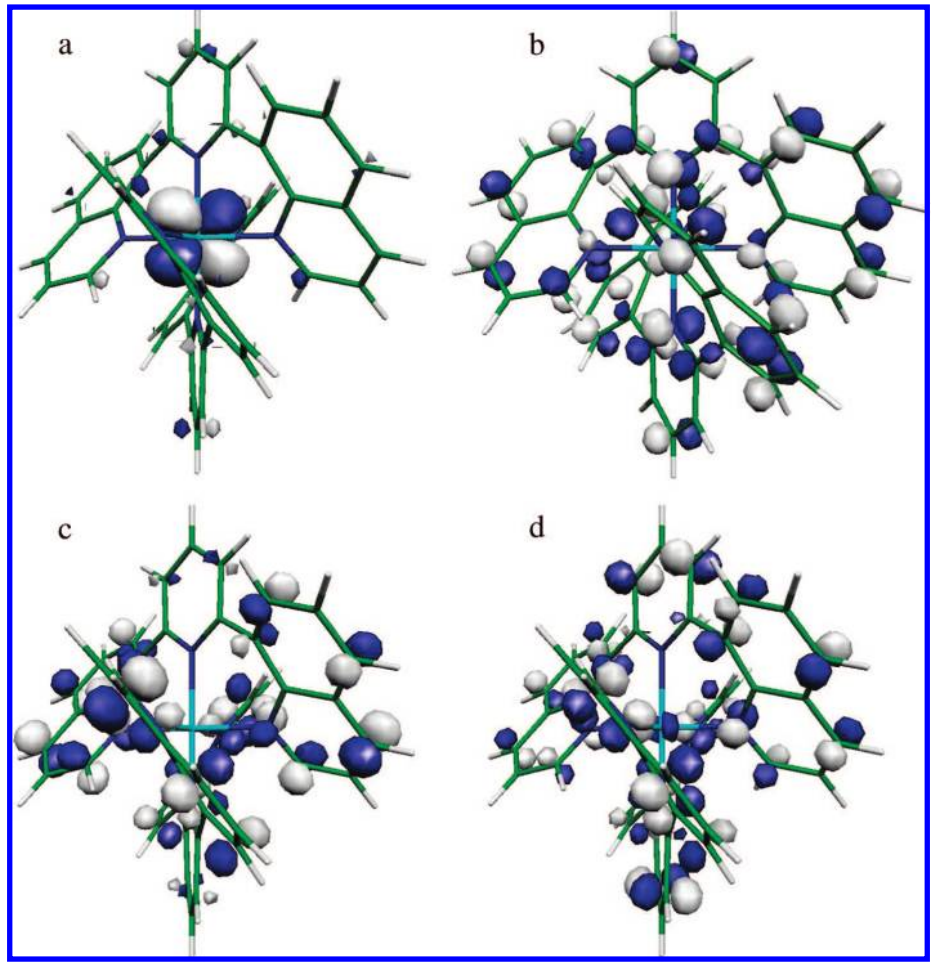

Figure 1. Molecular orbitals of **1** in EtOH according to B3LYP/LANL2DZ calculations with a PCM description of the solvent, with (a) HOMO, (b) LUMO, (c) LUMO+1, and (d) LUMO+2.

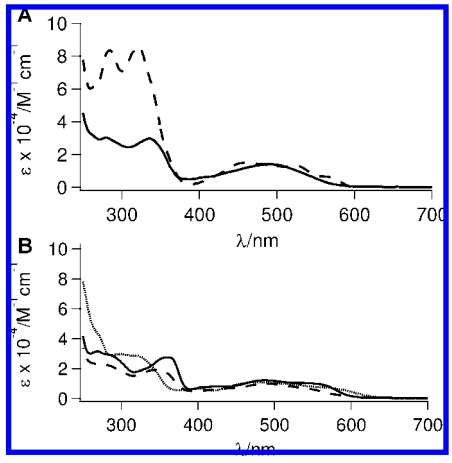

Figure 2. (a) Electronic absorption spectra of **1** (—) and **5** (---) in CH_3CN. (b) Electronic absorption spectra of **2** (---), **3** (••••), and **4** (—) in CH_3CN.

Table 3. Selected TD-DFT Calculated Vertical Singlet Excitations of **1** with B3LYP/LANL2DZ in a PCM Description of Ethanol, Performed on the B3LYP/LANL2DZ Gas Phase Optimized Geometry[a]

λ (nm)	*E* (eV)	*f*	assignment
538	2.30	0.042	MLCT
512	2.42	0.015	MLCT
502	2.47	0.082	MLCT
490	2.53	0.106	MLCT/MC
448	2.77	0.012	MLCT
446	2.78	0.095	MLCT
400	3.10	0.028	MLCT/MC
362	3.43	0.302	LC
337	3.69	0.129	LC/MLCT/LMCT

[a] Calculated excitation wavelengths (λ, nm), excitation energies (*E*, eV), oscillator strengths (*f*), assignments of the dominant contribution(s). Excitations with oscillator strengths exceeding 0.01 were included for excitations with wavelengths longer than 400 nm, and excitations with oscillator strengths exceeding 0.1 were included for excitations with wavelengths shorter than 400 nm.

with **2** showing an unprecedented ^{3}MLCT lifetime of 5.5 μs in Ar-purged EtOH/MeOH at 298 K (see Figure 3). The excited-state energies are still high, around 1.85 eV as estimated from the 0−0 emission maximum in EtOH/MeOH glass at 80 K (Figure 4). Also the lifetime for **3** of 0.45 μs is long considering that the comparatively low ^{3}MLCT energy leads to faster direct nonradiative decay to the ground state, according to the energy gap-law.[3a] Our results for **1**−**4** show for the first time that one can combine the favorable symmetry of bistridentate ruthenium(II) complexes with a long excited-state lifetime, even longer than those obtained in the best trisbidentate ruthenium(II) polypyridyl complexes.

As many of the favorable properties of ruthenium(II) polypyridyl sensitizers are dependent on the lowest excited-state being of ^{3}MLCT character, it is important to establish that not only the lowest absorption is a ^{1}MLCT transition (see above),

Table 4. Emission Maxima, Lifetimes and Quantum Yields, and Excited State Energies in Deoxygenated MeOH:EtOH Solution (1:4 by Volume)

	298 K			80 K			
	λ_{max} /nm	τ /μs	Φ_{em}	λ_{max} /nm	τ /μs	Φ_{em}	E_{00}[a]/eV
1	700	3.0	0.02	673	8.5	0.06	1.84
2	693	5.5	0.07	661	11.2	0.43	1.88
3	~780	0.45	$\sim 4 \times 10^{-4}$	726	2.7	0.007	1.71
4	706	4.3	0.04	672	10.7	0.22	1.85
5	685	7.4×10^{-3}	$< 5 \times 10^{-4}$	660	6.0	0.33	1.88
$[Ru(tpy)_2]^{2+}$[b]	–	0.25×10^{-4}	–	599	11.0	0.48	2.07
$[Ru(bpy)_3]^{2+}$[c]	630	1.0	0.089	582	5.1	0.33	2.13

[a] estimated from the emission maximum at 80 K as $E_{00} = 1240$ nm/λ_{max} (eV). [b] Data from ref 1c. [c] Data from ref 24 (data at 293 K) and ref 25 (data at 77 K).

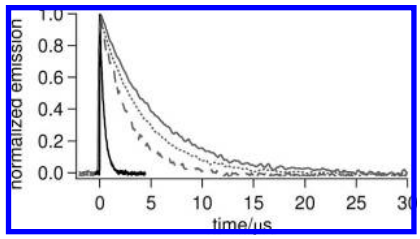

Figure 3. Emission decay traces for **1**−**4** after laser flash excitation in the lowest MLCT band: (dashed) **1**, (thin solid) **2**, (thick solid) **3**, and (dotted) **4**. Conditions: Ar-purged EtOH/MeOH at 298 K.

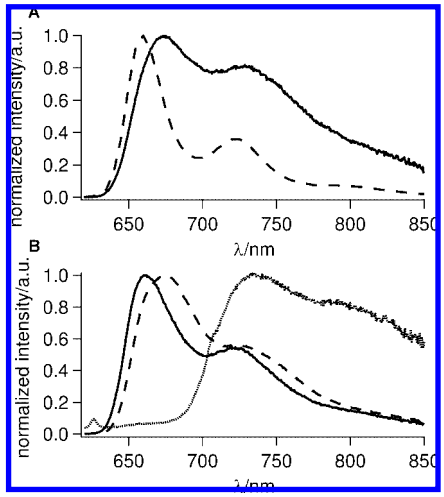

Figure 4. (a) Normalized and corrected steady state emission spectra of **1** (—) and **5** (---) at 80 K. (b) Normalized and corrected steady state emission spectra of **2** (---), **3** (····), and **4** (—) in EtOH/MeOH at 80 K.

but also that the thermally equilibrated, long-lived excited-state observed here is of MLCT nature, and not e.g. a ligand-centered triplet. This is also important in order to prove that the long emission lifetime reported above really is due to an intrinsically long-lived ^{3}MLCT state and not a delayed emission via a low-lying dark state. First, the in situ prepared $[Zn(dqp)_2]^{2+}$ complex, which should have a similar ligand conformation as in complex **1**, showed a room-temperature emission with maxima around 390 and 420 nm, which is much higher in energy than the emission of **1** (see Supporting Information of ref 9). Second, we note that the low temperature emission spectra of **1**−**5** in Figure 4 show the typical shape of ruthenium(II) polypyridyl ^{3}MLCT emission. Third, a linear relationship between the emission energy (E_{00}) and the difference in electrochemical potential between the first oxidation and reduction ($\Delta E_{1/2}$) is typical for MLCT states.[3b,26] Indeed, E_{00} and $\Delta E_{1/2}$ are shifted in parallel for the present complexes (cf. Tables 2 and 4). Thus,

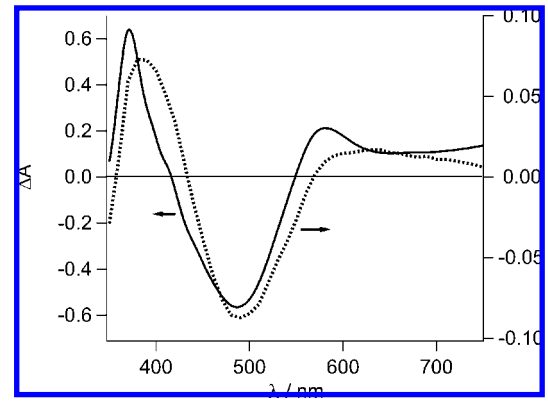

Figure 5. Transient absorption spectra of **1** at $t = 300$ ns (dashed line) in deoxygenated CH_3CN, and the sum of the difference spectra for spectro-electrochemical oxidation and reduction (solid line), in CH_3CN.

for **1**, **2**, **4**, and **5** E_{00} is 0.21 ± 0.02 eV lower and $\Delta E_{1/2}$ is 0.2 ± 0.1 V lower than the corresponding values for $[Ru(tpy)_2]^{2+}$. The values for **3** are also in agreement with this correlation, with E_{00} and $\Delta E_{1/2}$ being 0.36 eV and 0.34 V lower than for $[Ru(tpy)_2]^{2+}$, respectively. We note that this also supports the assignment of a metal-based first oxidation of **3** in the electrochemical experiments. Fourthly, transient absorption spectra of **1**−**4** (Figure 5 and Supporting Information) are in agreement with a ^{3}MLCT state[27] (the ^{3}MLCT lifetime of **5** was too short to be measured by ns flash-photolysis). The transient spectra decay with a uniform single-exponential rate constant over the spectral range 330 to 750 nm, which is equal to the emission decay rate constant, with several well-defined isosbestic points (see Supporting Information). Thus, there is no evidence for involvement of additional, nonemitting states in the decay of the thermally equilibrated ^{3}MLCT state. The transient spectra show the ground-state bleach features, weak absorptions in the red part of the spectrum, and a strong absorption around 350−400 nm. The latter is usually attributed to the reduced ligand absorption while the former is a mixture of reduced ligand $\pi-\pi^*$ absorption and ligand-to-metal charge transfer (LMCT) absorptions in the excited, formally $*[LRu^{III}L^-]^{2+}$, state.[3,27a] Furthermore, for **1** the shape of the transient spectrum is similar to the sum of the difference spectra for electrochemical oxidation and reduction of the complex (Figure 5). This has been shown

(24) Cook, M. J.; Lewis, A. P.; Mcauliffe, G. S. G.; Skarda, V.; Thomson, A. J.; Glasper, J. L.; Robbins, D. J. *J. Chem. Soc., Perkin Trans. 2* **1984**, 1293–1301.
(25) Watts, R. J.; Crosby, G. A. *J. Am. Chem. Soc.* **1972**, *94*, 2606–2614.
(26) Vlcek, A. A.; Dodsworth, E. S.; Pietro, W. J.; Lever, A. B. P *Inorg. Chem.* **1995**, *34*, 1906–1913, and references therein.
(27) (a) McCusker, J. K. *Acc. Chem. Res.* **2003**, *36*, 876–887. (b) Sun, H.; Hoffman, M. Z. *J. Phys. Chem.* **1993**, *97*, 11956–11959.

Table 5. Excited State Electron and Energy Transfer Data for **1** in CH_3CN

quencher[a]	ΔG^0/eV[b]	$k_q/ \times 10^9 M^{-1}s^{-1}$	quenching mechanism
MV^{2+}	−0.31	0.33	Oxidative (eq 1)
TTF	−0.15	9.9	Reductive (eq 2)
DPA	−0.13	3.4	Triplet energy transfer (eq 3)

[a] See text. [b] $\Delta G^0 = e(E^0_{Donor} - E^0_{Acceptor}) - E_{00}$, work terms were ignored. E_{00}(DPA) = 1.71 eV (ref 31), $E^0(MV^{2+/+}) = -0.820$ V vs $Fc^{+/0}$ (ref 32), $E^0(TTF^{+/0}) = +0.33$ vs. SCE (ref 33), 0.370 V was subtracted to obtain the value vs $Fc^{+/0}$. Data for **1** were taken from Tables 2 and 4.

to be a diagnostic feature of the ^{3}MCLT state for many Ru^{II}-polypyridine complexes[27a] although a perfect agreement cannot be expected as, for example, the different metal−ligand interactions are not independent of each other. In conclusion, all this data strongly support an assignment of the long-lived lowest excited-state in the series of complexes **1**−**5** to a ^{3}MLCT state.

In a more detailed photophysical report, submitted separately to a specialized journal, we show by temperature-dependent measurements that deactivation of the ^{3}MLCT state via higher lying ^{3}MC states is insignificant.[28] In sharp contrast, this activated process is responsible for the very short room temperature lifetimes of bistridentate complexes ($\tau = 0.25$ ns for $[Ru(tpy)_2]^{2+}$)[1c,2] and is very significant also for $[Ru(bpy)_3]^{2+}$ at room temperature.[3] The results thus confirm that our design strategy to increase the excited-state lifetime was successful: the larger bite angle of the dqp ligand compared to both tpy and bpy gives a more octahedral complex, as confirmed by X-ray crystallography, and this in turn is a useful way of substantially retarding deactivation via ^{3}MC states. In contrast, the lifetime for the heteroleptic **5** with one tpy ligand was only 7.4 ns, similar to the lifetime of our previously published complex $[Ru(bpy\text{-}CH_2\text{-}py)_2]^{2+}$ (bpy-CH_2-py is [6-(2,2′-bipyridyl)]-(2-pyridyl)-methane]) where each ligand gives one five- and one six-membered chelate ring.[12] Another homoleptic, mixed 5-/6-membered chelate complex by Thummel and coworkers, $[Ru(L)_2]^{2+}$ where L = 8-(1′,10′-phenanthrolin-2′-yl)quinoline, was very recently shown to have ^{3}MLCT lifetime of 810 ns,[29] partially due to destabilization of the ^{3}MC states and partially due to a lower ^{3}MLCT energy than in e.g. $[Ru(bpy\text{-}CH_2\text{-}py)_2]^{2+}$. Nevertheless, because these complexes were less octahedral than the present series of all 6-membered chelate complexes **1**−**4**, their lifetimes were not as high. In the present study it is worth pointing out that complex **1** shows a very long lifetime even at temperatures as high as 363 K ($\tau = 1.3$ μs), where even e.g. $[Ru(bpy)_3]^{2+}$ displays a lifetime of only c.a. 100 ns.[30] This property is an important advantage of the present complexes at the elevated temperatures that may be encountered in future solar energy conversion systems and other light-driven devices.

Photochemical Reactions. The ability of this class of complexes to photosensitize electron and energy transfer reactions was tested in excited-state reactions, using **1** as a representative member of the series. Emission quenching experiments were conducted in CH_3CN with a typical electron acceptor methyl viologen ($MV(PF_6)_2$), an electron donor tetrathiofulvalene (TTF) and a triplet energy acceptor diphenylantracene (DPA). Stern-Volmer plots of I_0/I or τ_0/τ were linear in the whole range investigated ($\tau_0/\tau \leq 5$ for MV^{2+}, $\tau_0/\tau \leq 10$ for TTF and DPA). The resulting second-order quenching rate constants were close to diffusion controlled for TTF and DPA, and somewhat slower for MV^{2+} (Table 5). Nanosecond transient absorption spectra on the same solutions showed the formation of the expected photoproducts (see Supporting Information), according to eqs 1−3:

$$^3[Ru(dqp)_2]^{2+} + MV^{2+} \rightarrow [Ru(dqp)_2]^{3+} + MV^{\bullet+} \quad (1)$$

$$^3[Ru(dqp)_2]^{2+} + TTF \rightarrow [Ru(dqp)_2]^{+} + TTF^{\bullet+} \quad (2)$$

$$^3[Ru(dqp)_2]^{2+} + DPA \rightarrow [Ru(dqp)_2]^{2+} + {}^3DPA \quad (3)$$

These results show that **1** is indeed a very useful sensitizer for these important types of photochemical reactions. As an illustrative contrast, while 3×10^{-5} M TTF is sufficient to obtain 50% quenching of excited **1**, it would quench a sensitizer with a lifetime of ≤1 ns, such as $[Ru(tpy)_2]^{2+}$ or $[Ru(ttpy)_2]^{2+}$, to at most 0.03%. Also in intramolecular reactions many systems based on ruthenium(II) polypyridyl show electron transfer reactions with rather modest rates ($k_{ET} < (1\text{ ns})^{-1}$)[1,34] so that intrinsic ^{3}MLCT lifetimes of at least a few hundred nanoseconds are necessary to obtain high electron transfer yields.

To assess the photostability of this new class of complexes, **1** was tested and compared with that of the common $[Ru(bpy)_3]^{2+}$. Irradiation of a solution of ruthenium(II) polypyridyl complexes commonly leads to ligand substitution, via population of metal-centered states.[3a,35] The photosubstitution yield for a complex depends strongly on e.g. the solvent and other potential ligands in the solution. The purpose here is not to examine the photosubstitution mechanism, but in a more practical sense to evaluate the stability of **1** in photochemical reactions under typical conditions. We noted no degradation at all during the emission experiments in EtOH/MeOH, although some samples were kept for days in sealed cells under frequent exposure to both ambient and experimental light. We then performed stability tests under more harsh conditions, in the presence of 2 mM chloride ions in air-equilibrated CH_2Cl_2 or CH_3CN. The photoanation quantum yield for $[Ru(bpy)_3]^{2+}$ under similar conditions in CH_2Cl_2 is reported as $\Phi = 0.068$.[35] The solutions were irradiated at 470 nm using the double monochromator (2 mm slits) and 450 W Xe-lamp of the fluorimeter. The stability of the complexes was judged from the emission intensity, as the photoproducts would show no or only weak photoemission. After 200 min of irradiation of the $[Ru(bpy)_3]^{2+}$ solution in CH_3CN only half of the initial emission remained. In contrast the solution of **1** maintained more than 90% of its initial intensity still after 800 min (>12 h; see Supporting Information). In CH_2Cl_2, the decomposition half-life of $[Ru(bpy)_3]^{2+}$ decreased

(28) Abrahamsson, M.; Becker, H.-C.; Hammarström, L. manuscript in preparation.
(29) Abrahamsson, M.; Becker, H.-C.; Hammarström, L.; Bonnefous, C.; Chamchoumis, C.; Thummel, R. P. *Inorg. Chem.* **2007**, *46*, 10354–10364.
(30) Van Houten, J.; Watts, R. J. *J. Am. Chem. Soc.* **1976**, *98*, 4853–4658.
(31) Murov, S. L.; Carmichael, I.; Hug, G. L. *Handbook of Photochemistry*, 2nd ed.; Marcel Dekker: New York, 1993.
(32) Lomoth, R.; Häupl, T.; Johansson, O.; Hammarström, L. *Chem.−Eur. J.* **2002**, *8*, 102–110.
(33) Coffen, D. L.; Chambers, J. Q.; Williams, D. R.; Garrett, P. E.; Canfield, N. D. *J. Am. Chem. Soc.* **1971**, *93*, 2258–2268.
(34) (a) Johansson, O.; Borgström, M.; Lomoth, R.; Palmblad, M.; Bergquist, J.; Hammarström, L.; Sun, L.; Åkermark, B. *Inorg. Chem.* **2003**, *42*, 2908–2918. (b) Borgström, M.; Shaikh, N.; Johansson, O.; Anderlund, M. F.; Styring, S.; Åkermark, B.; Magnuson, A.; Hammarström, L. *J. Am. Chem. Soc.* **2005**, *127*, 17504–17515. (c) Chaignon, F.; Falkenström, M.; Karlsson, S.; Blart, E.; Odobel, F.; Hammarström, L. *Chem. Commun* **2007**, *64*, 66.
(35) Durham, B.; Caspar, J. V.; Nagle, J. K.; Meyer, T. J. *J. Am. Chem. Soc.* **1982**, *104*, 4803–4810.

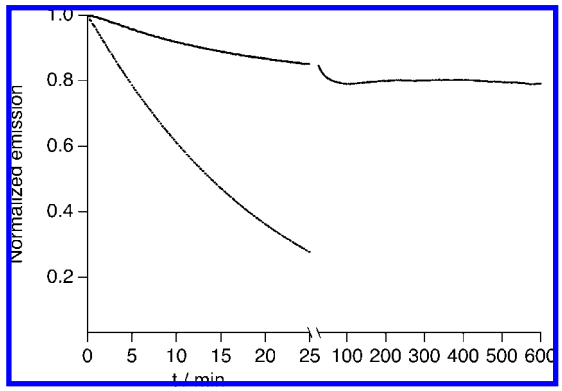

Figure 6. Photostability experiments, monitoring the decrease in emission intensity of the complex as a function of irradiation time in CH_2Cl_2 with 2 mM TBACl: **1** (upper line), $[Ru(bpy)_3]^{2+}$ (lower line).

to only 14 min (Figure 6), and the absorption spectrum was completely changed (not shown). Interestingly, the **1** emission decreased somewhat to c.a. 85% in 30 min, after which it remained constant for at least 600 min. The absorption spectrum showed correspondingly small changes. Preliminary analysis suggests that **1** can be reformed photochemically from the products, so that a photostationary state is reached after 30 min.[36] Of importance here is the remarkably high practical photochemical stability of **1**, which is a key asset for a sensitizer, in particular if it should be incorporated in more elaborate molecular arrays and in devices.

Conclusions

We have shown that the unusually large ligand bite angles of the dqp ligand give ruthenium(II) complexes with a close to perfect octahedral geometry. This results in a strong ligand field and hence substantially slower deactivation of the lowest ^{3}MLCT state via ^{3}MC states. Complexes **1**, **2**, and **4** show unprecedented ^{3}MLCT lifetimes, between 3.0 and 5.5 μs in room temperature solution, the longest ever reported for ruthenium(II) polypyridyl complexes. The substituted complexes **2**−**4** retain the favorable photophysical properties of the parent complex **1**, and are amenable for further functionalization with electron donor and acceptor units. Furthermore, the excited-state of **1** was shown to be a competent photosensitizer in bimolecular excited-state electron and energy transfer reactions with typical donors and acceptors. In addition, the photostability of **1** in solution is remarkably good, even under harsh conditions. Our results show for the first time that one can combine the favorable symmetry of bistridentate ruthenium(II) complexes with a long ^{3}MLCT excited-state lifetime and other favorable photosensitizer properties. Complex **1** and the derivatives **2**−**4** are therefore a promising starting point for the construction of linear, rod-like molecular arrays with applications in artificial photosynthesis and molecular electronics.

Experimental Section

Spectroscopy. NMR spectra were recorded on a JEOL 400 MHz spectrometer at 293 K. Chemical shifts are given in ppm and referenced internally to the residual solvent signal, all coupling constants (*J*) are given in hertz (Hz). UV−vis absorption spectra were measured on a Hewlett-Packard 8453 diode-array instrument or on a Varian Cary 50 UV−vis spectrophotometer. Measurements were done in 1 × 1 cm^2 quartz cuvettes. Molar absorption coefficients were determined in CH_3CN of spectroscopic grade.

All emission measurements were carried out in a 1:4 (v:v) MeOH:EtOH mixture in 1 × 1 cm^2 quartz cuvettes. Transient absorption measurements were carried out either in a 1:4 (v:v) MeOH:EtOH mixture or in acetonitrile of spectroscopic grade. Oxygen was removed by purging with argon in the cuvette before and during measurements. Emission spectra and yields at 80 K were measured in 1 × 1 cm^2 optical quartz cells in an Oxford Instruments liquid nitrogen cryostat DN1704 and the temperature was set with an Oxford Instruments ITC601 temperature controller. Emission lifetimes at 80 K was measured using a coldfinger setup in a liquid nitrogen filled dewar. Emission yields at room temperature were measured with $[Ru(bpy)_3]^{2+}$ in deoxygenated CH_3CN (Φ_{em} = 0.059[37]) and air-equilibrated EtOH/MeOH (Φ_{em} = 0.029[24]) as standards (both giving the same results). At 80 K, **1** was used as a standard (Φ_{em} = 0.062[9]) for complexes **2**−**5**.

Steady state emission measurements were performed on a SPEX Fluorolog II or Flourolog III fluorimeter, and corrected for wavelength sensitivity of the detector. Time-resolved emission and transient absorption measurements were performed using a Quantel Brilliant B Q-switched Nd:YAG laser and Opotek OPO producing <10 ns flashes at 410−690 nm. An Applied Photophysics LKS60 Laser flash photolysis spectrometer was used for detection, with a 150 W pulsed Xe-lamp providing analyzing light for transient absorption. The emission or transient absorption was detected at right angle with a monochromator and a P928-type PMT. The PMT output was recorded on a Hewlett-Packard digital oscilloscope (2 Gsamples/s, 500 MHz bandwidth) and analyzed with the Applied Photophysics LKS60 software. The instrument response time (risetime from 10−90% of a signal step) was <10 ns.

The excited-state lifetime of **5** was shorter than 10 ns and thus determined using a time correlated single photon counting setup. Excitation light was produced with a Coherent Mira Oscillator in a regeneratively amplified system. The frequency doubled output was used (400 nm) at a repetition frequency of 200 kHz. The emission was detected at magic angle and perpendicular to the excitation light. Blue filters were used to remove remaining 800 nm light in the excitation beam, and red filters were used to remove scattered light in the detection. The emitted light was collected by a MCP photomultiplier. Curve fitting of the data was performed using a nonlinear least-squares fitting procedure in IGOR Pro, version 5.04B.

Electrochemistry. Electrochemical experiments were performed as described elsewhere[34a] with a three-electrode setup in a three-compartment cell connected to an Autolab potentiostat with a GPES electrochemical interface (Eco Chemie). The working electrode was a glassy carbon disk (diameter 3 mm, freshly polished). Potentials were measured vs a nonaqueous Ag/Ag^+ reference electrode (CH Instruments, 10 mM $AgNO_3$ in CH_3CN) with a potential of −0.080 V vs the ferrocenium/ferrocene ($Fc^{+/0}$) couple in CH_3CN.

Calculations. Full geometry optimizations have been performed in the gas phase using density functional theory (DFT) calculations employing the B3LYP hybrid exchange-correlation functional[38] together with standard basis sets. Separate optimizations were performed in which the hydrogen, carbon, and nitrogen atoms were described using LANL2DZ, 6−31G, and 6−31+G(d,p), with LANL2DZ used for ruthenium in all cases.

Electronic excitations with wavelengths longer than ca. 300 nm were investigated using time-dependent DFT (TD-DFT) calculations performed on the gas-phase B3LYP/LANL2DZ optimized geometry using a polarizable continuum model (PCM)[37] to describe an ethanol solvent environment. All calculations were performed using the Gaussian03 program package.[39]

(36) Further studies of these reactions are in progress: (a) Kumar, R. J.; Jäger, M.; Johansson, O. manuscript in progress.

(37) Nakamuru, K. *Bull. Chem. Soc. Jpn.* **1982**, *55*, 1639.

(38) (a) Lee, C. T.; Yang, W. T.; Parr, R. G. *Phys. Rev. B* **1998**, *37*, 785. (b) Becke, A. D. *J. Chem. Phys.* **1993**, *98*, 5648.

(39) Frisch, M. J.; et al. *Gaussian 03*, revision B.05; Gaussian, Inc.: Wallingford, CT, 2003.

Synthesis. Microwave heating was performed in an Initiator single mode microwave cavity at 2450 MHz (Biotage). All commercially available reagents and solvents were used as received. $Ru(DMSO)_4Cl_2$,[40] the 2,6-di(quinolin-8-yl)pyridines,[9,14] and **1**[9] were prepared as described previously and $Ru(ttpy)Cl_3$ was synthesized in analogy to $Ru(tpy)Cl_3$.[41]

$[Ru(dqpCO_2Et)_2][PF_6]_2$ (2). A vial was charged with 4-ethylcarboxy-2,6-di(quinolin-8-yl)pyridine (70.0 mg, 0.173 mmol) and $RuCl_3 \cdot 3H_2O$ (21.0 mg, 0.081 mmol). After addition of EtOH (10 mL) and *N*-ethylmorpholine (0.2 mL), the tube was sealed and heated for 3 h at 80 °C. After the solution cooled to room temperature, aqueous NH_4PF_6 was added and the precipitate was filtered off and washed twice with H_2O and Et_2O. The crude product was purified by column chromatography on silica gel, using a mixture of CH_3CN/H_2O/sat. KNO_3 (~40:4:1) as the eluent. After concentration of the product containing fractions in vacuo and counterion exchange using NH_4PF_6 the solution was concentrated in vacuo to give **2** (19.5 mg, 0.016 mmol, 20%) as a red solid. ^{1}H NMR (CD_3CN): δ 8.27 (s, 4H), 8.09 (dd, J = 8.4, 1.5, 4H), 8.03 (dd, J = 8.1, 1.5, 4H), 7.79 (dd, J = 7.4, 1.1, 4H), 7.73 (dd, J = 8.4, 1.1, 4H), 7.50 (dd, J = 8.1, 7.7, 4H), 7.06 (dd, J = 8.1, 5.2, 4H), 4.46 (q, J = 7.2, 4H), 1.41 (t, J = 7.2, 6H); HRMS (ESI) m/z 1057.2214 $[M - PF_6]^+$ (calcd for $C_{52}H_{38}F_6N_6O_4PRu$ 1057.1640), 456.1392 $[M - 2PF_6]^{2+}$ (calcd for $C_{52}H_{38}N_6O_4Ru$ 456.0999).

$[Ru(dqpNH_2)_2][PF_6]_2$ (3). A 5 mL microwave tube was charged with 4-amino-2,6-di(quinolin-8-yl)pyridine (20.8 mg, 0.060 mmol) and $Ru(DMSO)_4Cl_2$ (14.3 mg, 0.030 mmol). After addition of ethylene glycol (2 mL), the tube was sealed and heated for 20 min at 200 °C in the microwave. The solution was cooled to room temperature, aqueous NH_4PF_6 was added, and the resulting precipitate collected by filtration and purified as for **2** to give **3** (7.0 mg, 0.006 mmol, 22%) as a red solid. ^{1}H NMR (CD_3CN): δ 8.17 (dd, J = 5.1, 1.4, 4H), 7.99 (dd, J = 8.1, 1.4, 4H), 7.60 (m, w = 16.5 Hz, 8H), 7.36 (dd, J = 8.1, 7.7, 4H), 7.07 (s, 4H), 7.04 (dd, J = 8.1, 5.1, 4H), 5.46 (s, br, 4H, NH_2); HRMS (ESI) m/z 943.1939 $[M - PF_6]^+$ (calcd for $C_{46}H_{32}F_6N_8PRu$ 943.1435), 399.1277 $[M - 2PF_6]^{2+}$ (calcd for $C_{46}H_{32}N_8Ru$ 399.0897).

$[Ru(dqp)(dqpCO_2Et)][PF_6]_2$ (4). 2,6-Di(quinolin-8-yl)pyridine (51.0 mg, 0.153 mmol) and $RuCl_3 \cdot 3H_2O$ (42.0 mg, 0.161 mmol) were suspended in EtOH (3 mL) in a sealed tube and heated at 100 °C for 24 h. The precipitate was filtered off, washed thoroughly with EtOH and Et_2O, and finally dried *in vacuo* at 50 °C to yield crude $Ru(dqp)Cl_3$ (70.0 mg). 4-Ethylcarboxy-2,6-di(quinolin-8-yl)pyridine (33.8 mg, 0.084 mmol), $Ru(dqp)Cl_3$ (45.9 mg) and 5 drops *N*-ethylmorpholine were suspended in EtOH (10 mL) in a sealed tube and heated for 24 h at 100 °C. After filtration of the crude reaction mixture, H_2O and EtOAc were added. The aqueous layer was washed once with EtOAc, separated and NH_4PF_6 and CH_2Cl_2 were added. The organic layer was concentrated under reduced pressure and the residue and purified as for **2** to give **4** (20.0 mg, 0.017 mmol, 20%) as a red solid. ^{1}H NMR (CD_3CN): δ 8.24 (s, 2H), 8.19 (t, J = 8.1, 1H), 8.06 (m, w = 27.5 Hz, 8H), 7.90 (d, J = 8.1, 2H), 7.73 (m, w = 38.5 Hz, 8H), 7.47 (m, w = 22.0 Hz, 4H), 7.05 (dd, J = 8.1, 5.1, 4H), 4.45 (q, J = 7.2, 2H), 7.04 (t, J = 7.2, 3H); HRMS (ESI) m/z 985.1230 $[M - PF_6]^+$ (calcd for $C_{49}H_{34}F_6N_6O_2PRu$ 985.1429), 420.0966 $[M - 2PF_6]^{2+}$ (calcd for $C_{49}H_{34}N_6O_2Ru$ 420.0893).

$[Ru(dqp)(ttpy)][PF_6]_2$ (5). 2,6-Di(quinolin-8-yl)pyridine (22.0 mg, 0.066 mmol), $Ru(ttpy)Cl_3$ (35 mg, 0.066 mmol) and N-ethylmorpholine (2 drops) were suspended in a mixture of EtOH (16 mL) and H_2O (4 mL). The mixture was refluxed for 12 h under a nitrogen atmosphere. After removal of excessive EtOH, aqueous NH_4PF_6 and CH_2Cl_2 were added. The organic layer was separated and concentrated *in vacuo* and the residue purified as for **2** to give **5** (20.0 mg, 0.018 mmol, 29%) as a red solid. ^{1}H NMR (CD_3CN): δ 8.68 (dd, J = 7.7, 1.1, 2H), 8.58 (s, 2H). 8.42 (dd, J = 8.4, 7.6, 1H), 8.33 (m, w = 7.3 Hz, 4H), 8.27 (dm, J = 8.1, 2H), 8.15 (dd, J = 8.4, 1.1, 2H), 7.99 (dd, J = 8.1, 1.1, 2H), 7.91 (d, J = 8.1, 2H), 7.80 (m, w = 17.6 Hz, 4H), 7.49 (d, J = 8.1, 2H), 7.28 (dd, J = 5.2, 1.4, 2H), 7.17 (m, w = 13.2 Hz, 2H), 6.98 (dd, J = 8.1, 5.2, 2H), 2.48 (s, 3H); MS (ESI) m/z 379.1 [0.5 $(M - 2PF_6)^{2+}$, 100], m/z 757.6 $[(M - 2PF_6)^+$, 10].

Acknowledgment. This work was supported by The Swedish Energy Agency, the Knut and Alice Wallenberg Foundation, the Swedish Foundation for Strategic Research, and the EU/Energy Network project SOLAR-H2 (FP7 contract 212508). The Swedish National Supercomputer Center (NSC) is acknowledged for provision of computing resources. P.P. thanks the Swedish Research Council (VR) and the Göran Gustafsson Foundation for financial support.

Supporting Information Available: ^{1}H NMR spectra for **2**−**5**, COSY and NOESY spectra of **5**, transient absorption spectra of **1**−**4**, transient absorption spectra of **1** with electron and energy donors and acceptors, results of photostability experiment with **1** and $[Ru(bpy)3]^{2+}$ in CH_3CN, complete ref 39. This material is available free of charge via the Internet at http://pubs.acs.org.

JA804890K

(40) Evans, I. P.; Spencer, A.; Wilkinson, G. *J. Chem. Soc., Dalton Trans.* **1973**, 204–209.
(41) Sullivan, B. P.; Calvert, J. M.; Meyer, T. J. *Inorg. Chem.* **1980**, *19*, 1404–1407.